

# External electric field control of THz pulse generation in ambient air

Wen-Feng Sun,<sup>1,2</sup> Yun-Song Zhou,<sup>1,2,\*</sup> Xin-Ke Wang,<sup>3</sup>  
and Yan Zhang<sup>1,2,\*\*</sup>

<sup>1</sup>Department of Physics, Capital Normal University, Beijing 100037 China

<sup>2</sup>Beijing Key Lab for Terahertz Spectroscopy and Imaging Beijing, 100037 China

<sup>3</sup>Department of physics, Harbin institute of Technology, Harbin 150006 China

\*263zys@263.net; \*\*yzhang@mail.cnu.edu.cn

**Abstract:** A theoretical model has been proposed to describe the dependence of the THz wave generated in a laser-induced air plasma on the external electric field. Using this model we predict the following, (i) previously observed results show that the THz pulse enhances linearly with the increase of the external field; (ii) the THz pulse varies as a cosine function with the angle between the direction of the external electric field and the polarization of the incident exciting beam; (iii) and the amplitude is proportional to the square of the intensity of the incident pulse in a low energy region. These predictions are validated by our experiment.

© 2008 Optical Society of America

**OCIS codes:** (320.7110) Ultrafast nonlinear optics; (350.5400) Plasmas.

---

## References and links

1. H. Hamster and R. W. Falcone, *Ultrafast Phenomena VII*, edited by C. B. Harris et al (Springer, New York, 1990).
2. H. Hamster, A. Sullivan, S. Gordon, W. White, and R. W. Falcone, "Subpicosecond, Electromagnetic Pulses From Intense Laser-Plasma Interaction," *Phys. Rev. Lett.* **71**, 2725 (1993).
3. H. Hamster, A. Sullivan, S. Gordon, W. White, and R. W. Falcone, "Short-pulse terahertz radiation from high-intensity-laser-produced plasmas," *Phys. Rev. E.* **49**, 671 (1994).
4. D. J. Cook and M. Hochstrasser, "Intense terahertz pulses by four-wave rectification in air," *Opt. Lett.* **25**, 1210 (2000).
5. M. Kress, T. Loffer, S. Eden, M. Thomson, and H. G. Roskos, "Terahertz-pulse generation by photoionization of air with laser pulses composed of both fundamental and second-harmonic waves" *Opt. Lett.* **29**, 1120 (2004).
6. T. Bartel, P. Reimann, M. Woerner, and T. Elsaesser, "Generation of single-cycle THz transients with high electric-field amplitudes," *Opt. Lett.* **30**, 2805 (2005).
7. X. Xie, J. Dai, and X. C. Zhang, "Coherent Control of THz Wave Generation in Ambient Air," *Phys. Rev. Lett.* **96**, 075005 (2006).
8. T. Loffler, F. Jacob, and H. G. Roskos, "Generation of terahertz pulses by photoionization of electrically biased air," *Appl. Phys. Lett.* **77**, 453 (2000).
9. A. Houard, Y. Liu, B. Prade, V. T. Tikhonchuk, and A. Mysyrowicz, "Strong enhancement of terahertz radiation from laser filaments in air by a static electric field," *Phys. Rev. Lett.* **100**, 255006 (2008).
10. C. D. Amico, A. Houard, S. Akturk, Y. Liu, J. Le Bloas, M. Franco, B. Prade, A. Couairon, V. T. Tikhonchuk, and A. Mysyrowicz, "Forward THz radiation emission by femtosecond filamentation in gases: theory and experiment," *N. J. Phys.* **10**, 013015 (2008).
11. Y. R. Shen, *The Principles of Nonlinear Optics* (University of California, Berkeley A Wiley-Interscience Publication, 1984).
12. M. Meljiek, E. M. Wright, and J. V. Moloney, "Femtosecond pulse propagation in argon: A pressure dependence study," *Phys. Rev. E* **58**, 4903 (1998).

## 1. Introduction

Terahertz (THz) waves are currently of great interest due to a wide array of practical applications that has attracted a lot of attention to their generation and modulation. Despite this, intense THz wave source technology is still far less developed than that of other frequency waves. Strong radiation at the THz frequency range was predicted in 1990 [1] to result from the electric fields commonly developed by free ions in plasma. This effect was subsequently observed in an experiment by Hamster et al. [2, 3]. In Hamster's experiment, an intense laser was focused on high-pressure air to produce a plasma. Further investigations have shown that a type-I beta barium borate (BBO) crystal inserted into the laser beam before its focal point apparently enhances the intensity of the THz wave radiation produced [4, 5, 6, 7]. The BBO crystal produces the second harmonic field when the fundamental laser beam is transmitted through it. Based on the four-wave mixing theory, this second harmonic field will interact with the fundamental laser field at the focal point where the ionized air forms a plasma and the THz pulse is generated. Upon removal of the BBO crystal from the device, the THz pulse intensity appears to become quite faint [4]. The remnant THz wave is due to the non-linearity characteristic of the waked plasma, which produces a weak second harmonic wave. In practice, however, the BBO crystal is easily damaged and is not used in many real-world THz wave applications (for instance the generation of THz wave in long distance and remote sensing diagnostics). Therefore, it will be valuable to find a way to enhance or even modulate the THz wave by manipulation of a plasma system without a BBO crystal. In 2000, Loffler et al. [8] observed the generation of THz waves in air with an external electric field. They found that the THz wave pulse was remarkably enhanced with an increase in the external field. This remarkable experiment, however, has not yet been verified experimentally or investigated theoretically. Recently, a PRL article [9] demonstrated experimental and theoretical researches on the terahertz generated in air plasma with electric field, since their theoretical analysis is based on the model of air plasma, furthermore, the existing expressions [10] was utilized.

In this paper, we propose a new theory that is based on the traditional nonlinear optics theory to treat the air plasma model. Not only the dependence of the amplitude of THz pulse on the external electric field may be explained but also some other predictions are obtained by the theory. And then, the above theoretical results are validated by our experiments.

This paper is arranged as follows: Section II describes the theoretical model and predictions made by the model. Section III displays the experimental results for the validation of the theoretical predictions and further discussion. Finally, a brief summary is given in Section IV.

## 2. Theoretical model and predictions

When a strong laser beam with frequency  $\omega$  is focused at a point in air, a plasma will be created and excited in the ionized air at the focal point. This case is detailed in Fig.1, in which the propagation and polarization directions of the laser beam are defined as the y and z directions, respectively, i.e.  $\mathbf{E}^{(1)} = E_0^{(1)} \exp(ik_y y - i\omega t) \hat{z}$ . According to the theory of non-linear optics, the second harmonic electric current generated in the air plasma system will obey the well-known expression [11]:

$$\mathbf{J}^{(2)} = \frac{i\rho^{(0)} e^2}{2\omega^2 m^2} \left[ \frac{1}{\omega} (\mathbf{E}^{(1)} \cdot \nabla) \mathbf{E}^{(1)} + \frac{1}{c} \mathbf{E}^{(1)} \times \mathbf{B}^{(1)} \right] + \frac{ie^2 (\nabla \rho^{(0)} \cdot \mathbf{E}^{(1)})}{m^2 \omega^2 (1 + \omega_p^2 / \omega^2)} \mathbf{E}^{(1)}. \quad (1)$$

where  $\mathbf{E}^{(1)}$  and  $\mathbf{B}^{(1)}$  denote the electric and magnetic fields of the fundamental laser beam,  $\omega_p = (4\pi e \rho^{(0)} / m)^{1/2}$  is the plasma frequency of the excited air plasma system, and  $\rho^{(0)}$  is the non-harmonic component of the charge density of the electron system in the ionized air. For a homogeneous plasma system,  $\nabla \rho^{(0)} = 0$  the last term in Eq. (1) disappears and consequently

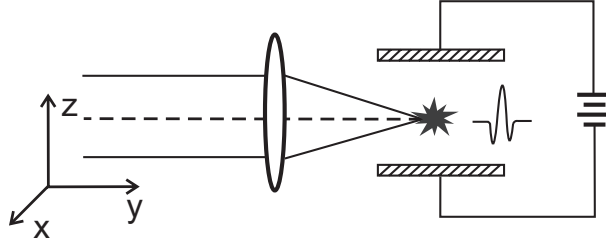


Fig. 1. Schematic plan of the setup used for THz generation controlled by an external electric field.

the second harmonic current is determined by the rest of the terms in Eq. (1). It is not difficult to see from the rest of the terms that the second harmonic current is along the  $y$ -direction, which cannot excite the  $y$  component of the second harmonic wave, thus there is no THz wave generated in the direction of observation. In general, a BBO crystal is inserted into the light path to generate a strong second harmonic wave so that a strong THz wave may be observed. In fact, when the BBO crystal is removed, a faint THz wave can still be observed. This is due to the size effect of the plasma system. In other words, in a finite system  $\nabla\rho^{(0)}$  will not be strictly zero.

We now assume that an electrostatic field  $\mathbf{E}_{ex} = E_{ex}\hat{z}'$  is applied to the plasma system (here  $\hat{z}'$  is a unit vector along an arbitrary direction). For a short time duration  $t$ , the electrons in the plasma will be accelerated suddenly and obtain the displacement  $\Delta z' = -eE_{ex}t^2/2m$ . This leads to the breakdown of homogeneity in the plasma system. The electron density will not only be related to the spatial position  $z'$ , but also to the displacement  $\Delta z' = -eE_{ex}t^2/2m$  or  $E_{ex}t^2$ , i.e.  $\rho^{(0)} = \rho^{(0)}(E_{ex}t^2, z')$ . In practice, the incident laser is a pulse of duration on the order of a femtosecond (fs), and thus  $E_{ex}t^2$  is a small quantity. The charge density may, therefore, be expanded in a power series with second order precision:

$$\begin{aligned} \rho^{(0)}(E_{ex}t^2, z') &= \rho^{(0)}(0, 0) + \frac{\partial}{\partial z'}\rho^{(0)}(0, z')_{z'=0}z' + \frac{\partial}{\partial E_{ex}t^2}\rho^{(0)}(E_{ex}t^2, 0)_{E_{ex}t^2=0}E_{ex}t^2 \\ &\quad + \frac{1}{2}\frac{\partial^2}{\partial z'^2}\rho^{(0)}(0, z')_{z'=0}z'^2 + \frac{1}{2}\frac{\partial^2}{\partial (E_{ex}t^2)^2}\rho^{(0)}(E_{ex}t^2, 0)_{E_{ex}t^2=0}(E_{ex}t^2)^2 \\ &\quad + \frac{1}{2}\frac{\partial^2}{\partial (E_{ex}t^2)\partial z'}\rho^{(0)}(E_{ex}t^2, z')_{E_{ex}t^2=0, z'=0}(E_{ex}t^2)z'. \end{aligned} \quad (2)$$

The second and fourth terms are zero since the charge density is homogeneous in the absence of an external field applied to the plasma system. The first, third, and fifth terms are not a function of spatial variables, so they cannot offer contributions to the gradient of the charge density. Then the leading term is the last term in Eq. (2):

$$\nabla\rho^{(0)} = \hat{z}' a E_{ex}. \quad (3)$$

Here:

$$a = \frac{1}{2}\frac{\partial^2}{\partial z'\partial E_{ex}t^2}\rho^{(0)}(E_{ex}t^2, z')_{E_{ex}t^2=0, z'=0}t^2. \quad (4)$$

Inserting Eq. (3) into Eq. (1) and canceling the former terms in Eq. (1), which do not contribute to THz waves in the direction of observation, the second harmonic current is thus:

$$\mathbf{J}^{(2)} = b \cos \theta E_{ex} \exp(2ik_y y - 2i\omega t) \hat{z}'. \quad (5)$$

where:

$$b = \frac{ie^2 a}{m^2 \omega^2 (1 + \omega_p^2 / \omega^2)} E^{(1)2}. \quad (6)$$

$\theta = \arccos(\hat{z} \cdot \hat{z}')$  is the angle formed by both the external field and the fundamental electric field, and  $E^{(1)} = |\mathbf{E}^{(1)}|$ . According to the non-linear theory, the second harmonic current can be regarded as a new driving current to produce the second harmonic electric field. For this purpose, the magnetic vector potential  $\mathbf{A}^{(2)}(\mathbf{r}, t)$  and scalar potential  $\varphi^{(2)}(\mathbf{r}, t)$  are employed. Considering the current continuity equation (for second harmonic charge density and current)  $\frac{\partial}{\partial t} \rho^{(2)} = \nabla \cdot \mathbf{J}^{(2)}$ , the second harmonic scalar potential has the form:

$$\varphi^{(2)}(\mathbf{r}, t) = \int_v \int_0^t \frac{\nabla \cdot \mathbf{J}^{(2)}(\mathbf{r}', t')}{|\mathbf{r} - \mathbf{r}'|} dt' d\mathbf{r}'. \quad (7)$$

It is easy to obtain the result from Eq. (5). Inserting this result into Eq. (7) we get  $\varphi^{(2)} = 0$  from Eq. (5). The second harmonic magnetic vector potential is expressed as:

$$\mathbf{A}^{(2)}(\mathbf{r}, t) = \frac{1}{c} \int \frac{\mathbf{J}^{(2)}(\mathbf{r}', t - |\mathbf{r} - \mathbf{r}'|/c)}{|\mathbf{r} - \mathbf{r}'|} d\mathbf{r}'. \quad (8)$$

Inserting Eq. (5) into Eq. (8), we obtain the expression:

$$\mathbf{A}^{(2)}(\mathbf{r}, t) = \frac{bE_{ex} \cos \theta}{c} I(\mathbf{r}) \exp(-i2\omega)\hat{z}. \quad (9)$$

$$I(\mathbf{r}) = \int \frac{\exp[i2k_y(y' + |\mathbf{r} - \mathbf{r}'|)]}{|\mathbf{r} - \mathbf{r}'|} d\mathbf{r}'. \quad (10)$$

Therefore:

$$\mathbf{E}^{(2)}(\mathbf{r}, t) = -\nabla\varphi^{(2)} - \frac{1}{c} \frac{\partial}{\partial t} \mathbf{A}^{(2)} = i2\omega \frac{bE_{ex} \cos \theta}{c^2} I(\mathbf{r}) \exp(-i2\omega)\hat{z}. \quad (11)$$

Equation (11) is the expression of the electric field of the second harmonic wave generated in the air plasma system, which will take part in the four-wave mixing process to generate the THz wave. According to the Four-wave mixing theory, the THz wave amplitude is related to the first and second harmonic fields as follows [4,5,7]

$$E_{THz} \propto E^{(1)2} E^{(2)}. \quad (12)$$

where  $E^{(2)} = |\mathbf{E}^{(2)}|$ . From Eqs. (6) and (11) and we see that  $E^{(2)}$  is proportional to  $E^{(1)2} E_{ex} \cos \theta$ . Substituting this relation into Eq. (12), we obtain the simple relation:

$$E_{THz} \propto E^{(1)4} E_{ex} \cos \theta. \quad (13)$$

Equation (13) reveals three characteristics: (i) The THz amplitude enhances linearly with an increase in the applied external electric field. This result has previously been observed experimentally [8]; (ii) The THz amplitude is proportional to the cosine of the angle between the wave vectors of the external field and the fundamental beam field; (iii) The THz amplitude is proportional to the biquadratic of the amplitude of the fundamental wave. The first of these characteristics is our main expected result, it predicts a new way to enhance the THz pulse or tune the THz amplitude. The second result also provides a simple method to control the THz amplitude by rotating the direction of the external field. The third one can also be written in terms of the incident energy  $I_\omega$  as:

$$E_{THz} \propto I_\omega^2. \quad (14)$$

In fact, this result was found earlier by Cook et al. in various experiments [4] and discussed in other literature [5, 6] In this paper, we obtained this result from our theoretical model.

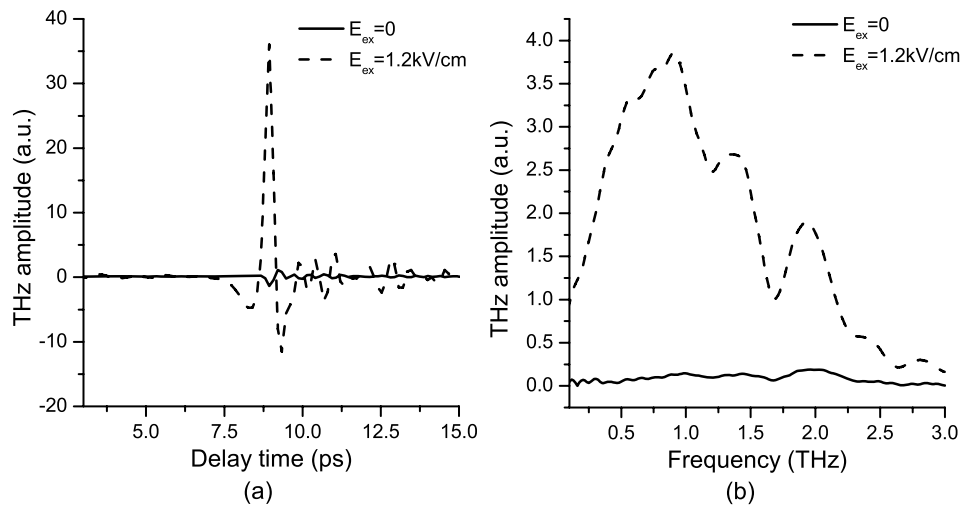


Fig. 2. The THz pulses generated in air plasma (a) and fourier transformed spectrums (b). The solid curve corresponds to a case without an external field and the dashed curve to the case of external field  $E_{ex} = 1.2\text{kV/cm}$  with  $\theta = 0^\circ$ .

### 3. Experimental results and discussion

Now we turn to the experimental validation of our theoretical predictions. The setup is expressed schematically in Fig. (1). The incident beam with a central wavelength of  $800\text{nm}$  and a pulse duration of  $50\text{fs}$  is focused in air by a convex lens with a focal length of  $150\text{mm}$ . The THz wave is detected by means of electro-optic sampling. In the focal region, where the peak intensity is  $1.6 \times 10^{15}\text{W/cm}^2$  at the pump energy of  $0.25\text{mJ}$ , there are two parallel plates separated from each other by a distance of  $D = 0.5\text{cm}$ . Electrodes applied to the plates can be supplied with a voltage varying from  $U = 0$  to  $6000\text{V}$ . The external field may be written as  $E_{ex} = U/D$ , which extends from  $E_{ex} = 0$  to  $1.2\text{kV/cm}$ . The pair of parallel plates may be turned around the principal optical axis of the convex lens so that the angle,  $\theta$ , between the direction of the external field and that of the electric field of the fundamental beam, may be changed.

In the experiment, the observed THz pulses generated in air plasma and their Fourier-transformed spectrums are given in Fig. (2). A faint background THz pulse is observed even without an external electric field as shown by the solid curve. The signal-to-noise ratio (SNR) is approximately 13. By applying an electric field along the direction of the electric field of incident beam ( $\theta = 0^\circ$ ) a much stronger THz pulse is measured and displayed by the dashed curve in Fig. (2). The peak value increases by about 32 times and the SNR increases about 13 times (from 13 to 175). We may conclude that the external field can enhance not only the peak of the THz pulse, but also the SNR.

By holding the angle  $\theta = 0^\circ$  constant and varying the value of the external field, different THz amplitudes are observed and displayed as the bars in Fig. (3). Each bar corresponds to the ten observed values and its thickness represents a difference of ten values. For example, the thickest bar, located at  $E_{ex} = 1.0\text{kV/cm}$ , which includes ten values that range from  $30.50$  to  $31.23\text{a.u.}$ , has a difference of  $\Delta A = 31.23 - 30.50 = 0.73(\text{a.u.})$ , so the measurement error is quite small. The straight line in Fig. (3) is linearly fitted using all of the amplitude values. We

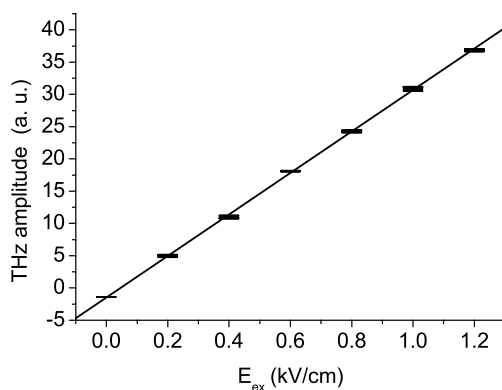


Fig. 3. Observed THz amplitudes (circles) generated in air plasma corresponding to different external fields  $E_{ex}$  when  $\theta = 0^\circ$ . The straight line is a curve of best fit for the amplitudes.

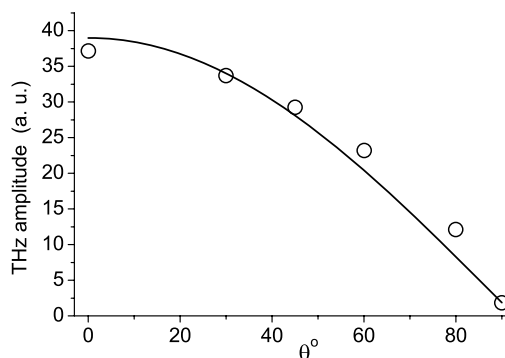


Fig. 4. Observed THz amplitudes corresponding to different rotation angles. The solid curve is a cosine form fitted to the observed amplitudes.

can see that all of the bars are close to the straight line so we conclude that the THz amplitude increases linearly with an increase of the external field. This result satisfies our prediction. The linear dependence was also described in the reference [9], nevertheless, we investigated the various rotation angles  $\theta$  significantly.

The THz amplitudes measured at various rotation angles  $\theta$  are displayed in Fig. (4). The circles express the experimental values, and the solid curve is a cosine fit curve. Figure (4) shows a clear relationship between the experimental results and the cosine curve. In other words, our second theoretical result is realized in this experiment. We also measured the THz amplitudes in the angle range from  $90^\circ$  to  $180^\circ$ , which also fit the cosine curve well. Lastly, we tested the relationship described by  $E_{THz} \propto I_\omega^2$ , where  $I_\omega$  is the laser pulse energy in the fundamental beam. The measured results are expressed with circles in Fig. (5). The solid curve is a quadratic curve fitted to the values in the low energy region, and the dashed straight line is the linear

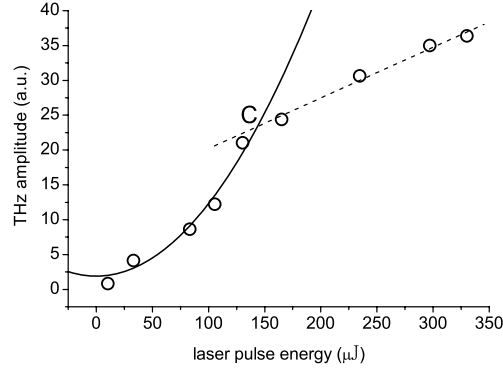


Fig. 5. Observed THz amplitudes corresponding to different laser pulse energies. The solid quadratic curve is fitted to the amplitudes in the low energy region.

curve fitted to the values in the high energy region. Fig.5 indicates that, in the low energy region, the relationship  $E_{THz} \propto I_{\omega}^2$  holds but that, in the high energy region, the THz amplitude falls below the quadratic fit curve. This phenomena has already been observed by Kress et al. and reported in Ref. 5, where it is described as a defocusing of the incident beam by plasma when the incident beam strikes with high energy [12]. The BBO crystal is used in Kress's experiment, but without an external field. Now we try to provide a perfect qualitative explanation of why the THz amplitude falls below the quadratic curve in the high incident energy region in experiment. According to the theory of non-linear optics, the charge density of the ionized air may be expressed as  $\rho = \rho^{(0)} + \rho^{(1)} + \rho^{(2)} \dots$  where  $\rho^{(1)}$  denotes the harmonic component of the charge density. As  $\rho^{(1)}$  oscillates with the same frequency as that of the incident beam, it is directly driven by  $\mathbf{E}^{(1)}$ . Consequently the assumption that  $\rho^{(1)}$  increases with the increase of the incident energy should be a reasonable one. When the incident energy is lower, the air plasma system is in an unsaturated state in which part of the air is unionized, so the variation of  $\rho^{(1)}$  with  $E^{(1)}$  will change the total charge density  $\rho$ , but it cannot influence  $\rho^{(0)}$  observably. In this case, Eq. (14) is validated. When the incident energy is so strong that the air plasma system goes over the saturated state, all air molecules are ionized and the total charge density  $\rho$  should reach its peak value and become a spatial constant. In this case an increase in  $\rho^{(1)}$  must lead to a decrease in  $\rho^{(0)}$ . As an increase of  $\rho^{(1)}$  is caused by an increase enhancement of incident energy, it is reasonable to assume that  $\rho^{(0)}$  is inversely proportional to the incident energy, i.e.  $\rho^{(0)} \propto 1/I_{\omega}$ . Thus Eq. (3) should be written as  $\nabla \rho^{(0)} = \hat{z} a E_{ex} / I_{\omega}$ . Inserting this relationship into Eq. (1) and then following all the above deductions, we find that Eq. (14) becomes:

$$E_{THz} \propto I_{\omega}. \quad (15)$$

Equation (15) just corresponds to the dashed line in Fig. (5). This explanation supports the idea that the intersection of the solid line and the dashed line (marked with C in Fig. (5)) is the critical point that divides the air plasma system into unsaturated and saturated states.

#### 4. Conclusion

Based on the non-linear theory of plasma and four-wave mixing theory, we proposed a theoretical model to describe the THz pulse generated in air by applying an external electric field. Our

theoretical deduction predicts that the THz amplitude increases linearly with the value of the external field (previously observed in the experiment), varies as a cosine function with the rotation angle, and is proportional to the square of the incident pulse intensity. These predictions have been validated by our experiment.

### **Acknowledgments**

The authors gratefully acknowledge Prof. Jing-Ling Shen and Cun-Lin Zhang for fruitful discussion. This work is supported by the Chinese National Key Basic Research Special Fund under Grant No. 2006CB302901 and the Development Foundation of Beijing Education Commission, China (Grant No. KM200710028006 and KM200810028008).